Audio Engineering Society

Convention Paper

Presented at the 130th Convention
2011 May 13–16 London, UK

Losses in Loudspeaker Enclosures

Claus Futtrup

Scan-Speak A/S, Videbæk, DK-6920, Denmark
~~cfu@scan-speak.dk~~
cfuttrup@gmail.com

ABSTRACT

In recent papers, a lumped parameter model, which can simulate the impedance of conventional electro-dynamic transducers accurately, has been presented. The new model includes frequency-dependent damping, which questions traditional engineering practices in simulations of loudspeaker enclosures and, in particular, associated losses. In this paper, the consequences of frequency-dependent damping are evaluated to aid the development of simulations and models of loudspeaker enclosures.

1. INTRODUCTION

In the circuit representing the motional impedance of a transducer, the damping in a transducer is traditionally represented by R_{ES}, a resistor in parallel to C_{MES} (representing the mass) and L_{CES} (representing the compliance), according to the lumped parameter model suggested by Thiele/Small.

Frequency-dependent damping due to $R_{AES} = \omega \cdot R_{AMS} = \omega \cdot (Bl)^2 \cdot A_{MS}$ (see *Fig. 1*) is introduced in the paper by Thorborg, et al. [1] as a method of representing visco-elastic effects at higher frequencies. Changes in compliance and creep effects are ignored and the focus is entirely on damping at audible frequencies, including the behavior of the transducer when mass is added and/or the transducer is placed in an enclosure (changes in system compliance).

In this paper, the influence of transducer frequency-dependent damping on the understanding of absorption losses in enclosures is clarified for the development of more accurate simulations of loudspeaker enclosures.

2. DAMPING AND Q-VALUES

Determining the Q-values of a transducer represented by the model in the paper by Thorborg, et al. ([1], *Fig. 6*), shown here in *Fig. 1*, cannot be executed simply by applying the same equations as those used in the Thiele/Small model. Q_{MS} must include the effect of R_{AMS}, and Q_{ES} must include the effect of the improved inductance model in the paper by Thorborg, et al. [2]. Instead, it is necessary to evaluate Z_E, the electrical component of the model, and the mechanical component, Z_{EM} (see *Fig. 1*).

The resonance frequency, when including R_{AMS} and the effects of the inductance model, is difficult to derive and assumes a complex value. Given a specific model of a transducer, the resonance frequency can be more easily determined using numerical iteration to trace the impedance maximum. Neglecting the influence of the inductance but including the effect of R_{AMS}, the following formula is given:

$$f_S = \sqrt{\frac{L_{CES} + jR_{AMS}}{4\pi^2 \cdot C_{MES}(L_{CES}{}^2 + R_{AMS}{}^2)}} \qquad (1)$$

To explain the importance of R_{AMS} with respect to enclosure losses, a low-damping transducer is used as an example. Likewise, since the results are not heavily dependent on an exact value of f_S, the resonance frequency can alternatively be defined in the following familiar way:

$$f_S = \frac{1}{2\pi \cdot \sqrt{C_{MES} \cdot L_{CES}}} \qquad (2)$$

Equation 2 is derived from Equation 1 by setting R_{AMS} = 0 and is approximately valid when $L_{CES} >> R_{AMS}$, neglecting the influence of the inductance. Any value of $R_{AMS} > 0$ will reduce the value of f_S, and inclusion of the inductance will increase the value of f_S.

Generally, this simplification works well. For low-damping transducers (high Q_{MS}), the simplified calculation of f_S is close to the true value of f_S. For high-damping transducers (low Q_{MS}), the simplified f_S can be a few percent off from the true value, but because the impedance peak is broader for low-damping designs, $R_{ES}'(f_S)$ will be close to the true value. If a small error is acceptable, the simplified equation can be used for designs with fairly high damping as well.

The total mechanical damping, with R_{ES} and R_{AMS} combined and therefore including both frequency-dependent and frequency-independent damping, is represented by R_{ES}':

$$R_{ES}'(f_S) = \mathrm{Re}\{Z_{EM}(f_S)\}$$
$$= \mathrm{Re}\left\{\left(\frac{1}{Z(C_{MES})} + \frac{1}{R_{ES}} + \frac{1}{Z(R_{AMS}, L_{CES})}\right)^{-1}\right\} \qquad (3)$$

When applying the traditional lumped parameter model as suggested by Thiele/Small, the R_{ES} value will be the same value as $R_{ES}'(f_S)$ in Equation 3.

The Q-values are determined as follows, starting with Q_{MS}:

$$Q_{MS}(f_S) = R_{ES}'(f_S) \cdot 2\pi \cdot f_S \cdot C_{MES}$$
$$\left(= R_{ES}'(f_S)/(2\pi \cdot f_S \cdot L_{CES})\right) \qquad (4)$$

Either L_{CES} or C_{MES} in Equation 4 can be used to determine Q_{MS}, if the simplified definition of f_S is used.

However, if the determination of f_S includes frequency dependent damping (in either a numerical or analytical way), it is recommended that C_{MES} be used to circumvent the influence of R_{AMS}.

When applying the advanced inductance model, the resistive part of the impedance, R_E, is a function of ω, which means that $R_E \neq R_{DC}$. Furthermore, the resistive component $R_E' \geq R_{DC}$ is given.

$$R_E(f_S) = \mathrm{Re}\{Z_E(f_S)\} = R_E' + \mathrm{Re}\left\{\left(\frac{1}{Z(L_E)} + \frac{1}{R_{SS}} + \frac{1}{Z(K_E)}\right)^{-1}\right\} \quad (5)$$

Q_{ES} is calculated with the R_E of Equation 5 and the lumped R_{ES}' of Equation 3:

$$Q_{ES}(f_S) = Q_{MS}(f_S) \cdot \frac{R_E(f_S)}{R_{ES}'(f_S)} \quad (6)$$

Q_{TS} is defined in the usual manner:

$$Q_{TS}(f_S) = \left(\frac{1}{Q_{MS}(f_S)} + \frac{1}{Q_{ES}(f_S)}\right)^{-1} \quad (7)$$

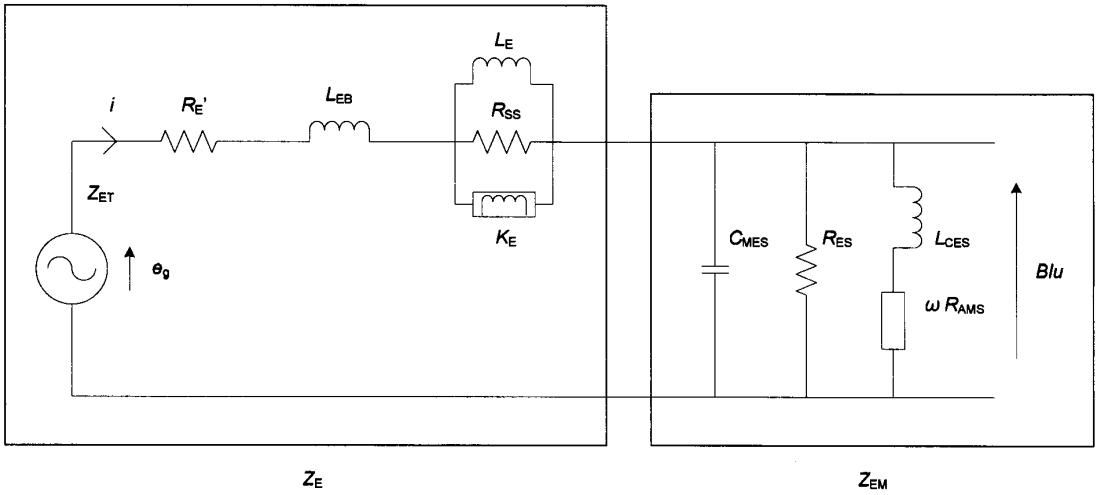

Figure 1 The model evaluated in the papers by Thorborg, et al. [1, 2] for a conventional electro-dynamic transducer incorporating frequency-dependent damping represented by R_{AMS} and an advanced inductance model, which includes semi-inductance and the effects of conductive elements near the voice coil in the magnet system represented by R_{SS} (semi-inductor shunt resistor).

2.1. Change of Damping with Change in Frequency

The frequency-dependent damping, defined by $R_{AES} = \omega \cdot R_{AMS}$ [Ω], is inversely proportional to the frequency. A quick study shows that the influence of R_{AES} increases at lower frequencies. The impedance of R_{AES} is special in that its change with frequency follows the impedance of the series inductor L_{CES}, representing the suspension compliance. If a steady-state sine-wave signal is applied above the resonance frequency, the transducer is mass-

controlled, and the majority of the current in the circuit (*Fig. 1*) goes through C_{MES}.

If a steady-state sine-wave signal is applied below the resonance frequency, the transducer is suspension-controlled, and the majority of the current flows through $L_{CES} + R_{AMS}$, which becomes increasingly important as the applied frequency of the signal is reduced. The power loss $P = R_{AES} \cdot i^2$ increases; hence, the frequency dependent damping increases as the frequency decreases.

This behavior is also valid for modern low-damping (high Q_{MS}) designs; it is the frequency-dependent damping (R_{AMS}) that is dominant over the frequency-independent damping (R_{ES}). This is shown with an example in Section 2.2.

2.2. Example Scan-Speak 18W/4531G00

The parameters in Table 1 describe the 18W/4531G00 transducer used in this study according to the model in *Fig. 1*.

The determination of M_{MS} using the advanced added mass technique follows the description in the paper by Thorborg, et al. ([1], Section 2.1) but without a laser velocity measurement. In this case, the data were obtained by curve-fitting them to two impedance measurements, with and without the added mass (see Thorborg, et al. [2], Section 2.0). The quality of the model can be evaluated by comparing the measured data to the simulated data (see *Fig. 2*).

Much effort was directed toward fitting the magnitude and phase around the resonance frequency (with and without added mass) down to -3 dB for the best possible determination of R_{ES} and R_{AMS}. Further efforts were focused toward determining the minimum impedance Z_{min} at f_{min} and properly fitting the value to the inductance (blocked impedance) at higher frequencies while attempting to work around the cone resonance at 750 Hz. Using a velocity laser provides a more direct way of determining *Bl* (see *Fig. 1*, where u = velocity), but a laser was not used in this case.

R_E'	3,44 Ω	M_{MS}	= 17,2 gram = $\Delta M \cdot C_{MES} / \Delta C_{MES}$		Adv. added mass
L_{EB}	0,0847 mH	Bl	= $\sqrt{}$ (M_{MS} / C_{MES}) = 4,87 Tm (or N/A)		
K_E	0,0189 SH	R_{MS}	= $(Bl)^2 / R_{ES}$ = 0,134 kg/s		
R_{SS}	92,5 Ω	f_S	= 1 / (2 π $\sqrt{}$ ($C_{MES} \cdot L_{CES}$)) = 33,8 Hz		(Numerical: 33,6 Hz)
L_E	1,74 mH	C_{MS}	= 1 / ($M_{MS} \cdot (2 \pi f_S)^2$) = 1,28 mm/N		
C_{MES}	727 uF	A_{MS}	= $R_{AMS} / (Bl)^2$ = 0,000194 s^2/kg (or m/N)		Admittance
R_{ES}	177 Ω	S_D	= 154 cm^2		
L_{CES}	30,5 mH			$R_{ES}'(f_S)$	= 34,7 Ω
R_{AMS}	4,59 mΩ · s			$Q_{MS}(f_S)$	= 5,36

Table 1 Parameters for the 18W/4531G00 transducer, preliminary data.

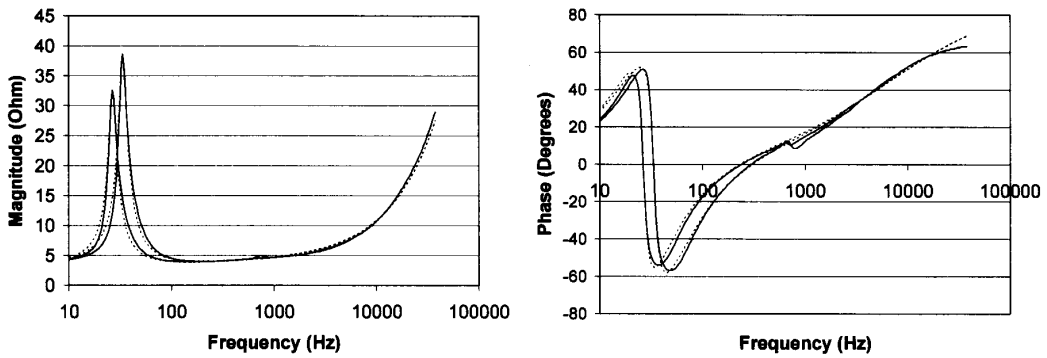

Figure 2 The measured free-air impedance of the 18W/4531G00 transducer (solid line) with and without added mass. The dashed curves represent simulated data fitted with the model in Figure 1. For actual verification of the quality of the fit one could view the calculated motional impedance separately (and perhaps even the Nyquist plot) to assure proper separation of electrical versus motional impedance.

To demonstrate the increasing damping at lower frequencies versus Q_{MS}, the model parameters of the 18W/4531G00 transducer example is changed by doubling M_{MS} and reducing M_{MS} to half of its original value, which is a theoretical approach to changing the resonance frequency f_S of the transducer without changing the suspension in any way. See Table 2 for results.

M_{MS} = 8,6 gram	(C_{MES} = 364 µF)	
	f_S	= 47,8 Hz
	$R_{ES}'(f_S)$	= 45,4 Ω
	$Q_{MS}(f_S)$	= 4,96
M_{MS} = 34,5 gram	(C_{MES} = 1455 µF)	
	f_S	= 23, 9 Hz
	$R_{ES}'(f_S)$	= 26,0 Ω
	$Q_{MS}(f_S)$	= 5,68

Table 2 The model of 18W/4531G00 modified with different moving masses.

R_{ES}' drops significantly for lower frequencies, reflecting the increase in damping. The change in Q_{MS} is small (± 7 %) because damping ($1/R_{ES}'$) is inversely proportional to the resonance frequency (when changing mass), and frequency dependent damping is dominant.

If the traditional lumped parameter model suggested by Thiele/Small had been used, Q_{MS} would have doubled from 3,8 to 7,6. This shows that the traditional model, when utilizing only frequency-independent damping represented by R_{ES}, would make Q_{MS} heavily frequency dependent. The impedance peaks of the simulated curves of *Fig. 2* would be of the same height, which would not correlate with the measured data.

Returning to the 18W/4531G00 transducer with M_{MS} = 17,2 grams. If R_{AMS} is neglected (zero) and R_{ES} remains unchanged, Q_{MS} = 27,4. If R_{ES} is neglected (infinity) and R_{AMS} remains unchanged, Q_{MS} = 6,63, which is much closer to the Q_{MS} value with both losses included.

Therefore it can be seen that, R_{AMS} is the dominant contribution to mechanical damping around f_S.

The example illustrates that the influence of R_{AMS} increases as the frequency of investigation is lowered and that the influence of R_{AMS} is expected to be larger than R_{ES} for a low-loss (high Q_{MS}) transducer design. This effect is expected to be even more pronounced for high-loss designs.

Finally, the resonance frequency is calculated in three different ways (see Table 3).

It can be seen that there is little difference between the calculated values. The values for the resonance frequency are within a few tenths of a Hertz from one another, and the values for the impedance peak differ only by a few hundredths of an ohm.

In this particular example, the advanced equation (Equation 1) produces a value closer to the numerical result. This is because the chosen transducer utilizes conductive short-circuiting devices in the magnet system near the voice coil, which reduces the overall inductance and is combined with a relatively low resonance frequency. A higher inductance could alter the result in favor of the simple equation (Equation 2). The advanced equation always predicts f_S lower than the true value.

Simple equation for f_S (neglecting inductance):	f_S = 33,81 Hz	Z_{RES} = 38,38 Ω
Advanced equation for f_S, real part (neglecting inductance):	f_S = 33,53 Hz	Z_{RES} = 38,42 Ω
Numerical iteration (including inductance):	f_S = 33,64 Hz	Z_{RES} = 38,44 Ω

Table 3 Numerical solution versus simplified equations for determination of the resonance frequency f_S.

3. ENCLOSURES WITH LOSSES

Small ([3], page 367) presented the results of a detailed analysis on enclosure losses. He found that absorption losses are fairly low, typically in the range of Q_A = 30–80 and for an unlined enclosure 100 or more, which can be neglected. Leakage losses are typically found in the range of Q_L = 5–20. Small observed inconsistency between these findings and his expectations. He states that this "...leads to the conclusion that the measured leakage in apparently leak-free systems is not an error of measurement but an indication that the actual losses in the system enclosure are not constant with frequency."

Small is very observant and holds that it is a fact that there is a frequency-dependent loss. With the introduction of R_{AMS}, the focus can be shifted from the enclosure to the transducer itself. It is the influence of R_{AMS} that causes the (somewhat) surprising observations, but the question remains whether enclosure damping is also frequency dependent. Nevertheless, since Small published his papers approximately 40 years ago, loudspeaker system designers have used the lumped parameter model suggested by Thiele/Small and have assumed Q_L = 7 as a general guideline.

With the introduction of R_{AMS} into the model of the transducer, it can no longer be assumed that leakage is in the vicinity of Q_L = 7 and absorption losses in the enclosure cannot be neglected.

Absorption losses due to damping material in an enclosure are more important above f_{SB} and less so below f_{SB} (see the paper by Small [3], *Fig. 4*), whereas the frequency-dependent damping of the transducer increases as the frequency decreases. These two effects partially balance out. Hence, Small has essentially observed the effect of the combined losses converted into leakage loss in his analysis.

To apply the lumped parameter model shown in *Fig. 1*, it is recommended that engineering practices change from relying on rules of thumb to relying on a physical model to determine absorption losses and obtain more accurate box simulations.

3.1. Modeling Absorption Losses

Absorption losses in enclosures are a combination of wall absorption in an unlined box, thermal effects of the fill material, and the mechanical properties of the fill material, such as aerodynamic flow resistance and added mass loading from the fiber fill onto the transducer.

The thermodynamic absorption provided by the fill material is a low-frequency process. At high frequencies, the behavior is essentially adiabatic, whereas below a certain cross-over frequency, the process becomes increasingly isothermal. When operating under an isothermal condition, the fill material provides a damping effect and an apparent volume expansion that is often explained by a reduction in sound speed in the medium, which stems from a change in the ratio of specific heats, γ, from that of air alone to that of a combination of the air and filling material.

The mechanical damping provided by the fill material is partially an effect of flow resistance, traditionally modeled as a porous material, and partially an effect of damping in the fiber material and friction between the fibers, which is a function of damping modulus, mass, compliance (modulus of elasticity) and coefficient of friction. Some of these effects may be neglected.

A model that could be suitable is the one developed by Leach [4], with corrections by Putland [5, 6]. This model is shown in *Fig. 3*, in which the original mechanical analogy is maintained, but the nomenclature is in accordance with this presentation. Neglected effects are crossed out.

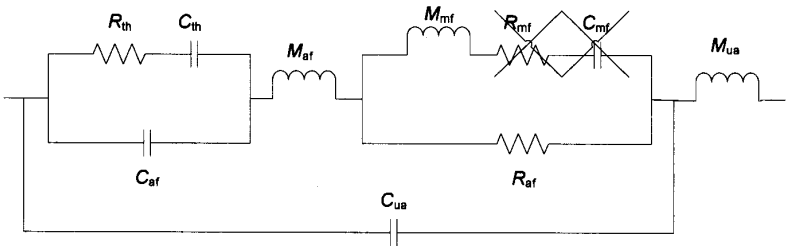

Figure 3 Combined electroacoustic-analogous circuit modeling both thermodynamic effects and mechanical parameters of filling in filled, closed box (see the paper by Leach [4], Fig. 6), which is expanded with components representing the unfilled section.

In the mechanical analogy, *Fig. 3*, C_{af} represents the mechano-acoustic compliance of the air (in the fiber-filled area), M_{af} the aerodynamic mass load of the air on the transducer (in the fiber filled area) and R_{af} the aerodynamic flow resistance through the damping material (Putland: Viscous interaction between the fibers and the air). R_{th} and C_{th} represent the thermodynamic effects. M_{mf} represents the mass of the fibers, R_{mf} the mechanical damping and C_{mf} the compliance of the fibers. The model represents an enclosure section filled 100 % with damping material. The unfilled section of the enclosure is represented by mass loading M_{ua} and compliance C_{ua}.

In many real-world situations, damping only partially fills the enclosure. If the equations by Leach [4] and Putland [5] are applied without accounting for the fact that these papers only consider enclosures that are 100 % filled with uncompressed damping material (m = 20 for the treated example of glass wool; Putland makes a short note about this), false results will be produced. A small quantity of damping material, for example, a small amount of dust in the air, can expand the enclosure volume by 3 %, and a few grams of damping material can expand the enclosure volume by as much as 10 %. These clearly unrealistic findings arise when the equations are applied careless. It is also assumed that the fibrous material fills the entire enclosure evenly, no matter how low the density becomes, resulting in incorrect values for the enclosure expansion and damping. Instead, one must be sure that the fill factor f and time constant τ_{fp} correspond to real values and that these only affect the part of the volume filled with damping material.

Putland described in his PhD thesis [6] a finite-difference equivalent circuit (FDEC) method for calculating an enclosure that can be filled or partially filled with damping material. The method can include geometric aspects of the enclosure and the location and size of the transducer and damping material. A finite-difference model is a simple alternative to real finite-element models, and Putland has shown how relatively few circuits in a mesh can describe a situation up to an arbitrary selected upper frequency, with each circuit representing a volume element. Such a model is more accurate than the lumped parameter model treated here, which is a simplification that is unable to predict higher-

order effects, such as those due to internal resonances in the enclosure. It is also unable to calculate uneven distributions of the damping material – the compression of the damping material is a fixed value across the entire filled part of the enclosure. In addition, the filled part is a percentage of the volume and considered to be in contact with the walls by the same percentage, as well as influencing the driver by this percentage.

Furthermore, Putland's PhD thesis shows that the low-frequency effects of adding damping material are generally undesirable side effects. The purpose of the damping material is to limit the effects of standing waves (acoustic modes) in the enclosure on the acoustic output.

The lumped parameter model treated here is illustrated in *Fig. 4* with all components converted to their electrical equivalents.

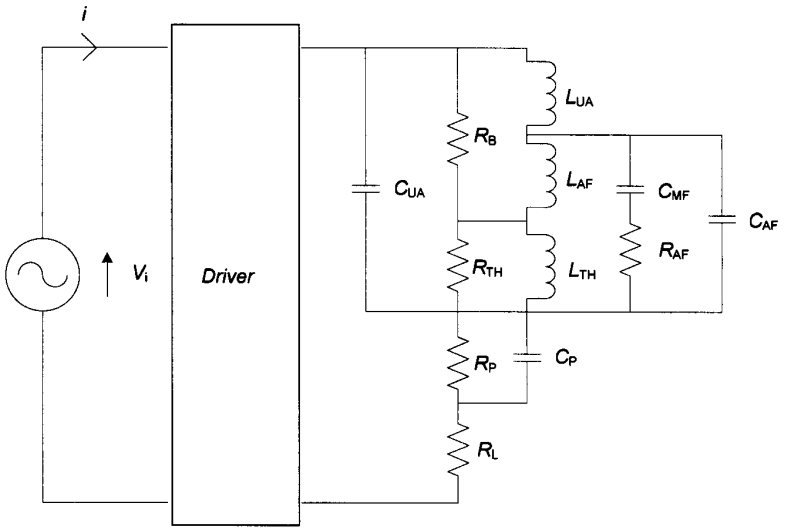

Figure 4 Model of enclosure with losses. The box titled "Driver" can contain, for example, the transducer model of Fig. 1. The above model contains C_P and R_P for the port mass and port loss of a reflex box – these are to be removed to simulate a closed box. If the simulation of a passive radiator system is desired, the model can be expanded with L_{CES} and R_{AMS} for the passive radiator. Port and leakage are not treated any further in this paper.

In *Fig. 4*, the air volume is symbolized by two inductors, L_{UA} and L_{AF}, representing the unfilled and the filled part of the volume, respectively. Wall absorption is symbolized by R_B. Thermodynamic volume expansion and absorption are symbolized by L_{TH} and R_{TH}, respectively. The air mass load on the transducer for the unfilled and filled parts is represented by two capacitors, C_{UA} and C_{AF}, respectively. Finally, the mass

load of the fiber fill on the driver and aerodynamic flow resistance are symbolized by C_{MF} and R_{AF}, respectively.

It can be seen that both the volume of the air and the mass load of air in the enclosure are represented by two components each. One of each element will become zero when the enclosure is either unfilled or completely filled with damping material.

The model in *Fig. 4* is in agreement with the model by Leach when neglecting the compliance of the fiber, C_{mf}, and mechanical damping, R_{mf}, also named "damping resistance" by Leach (both are crossed out in *Fig. 3*). The reason for doing so is given by Putland [6]. He analyzed the established FDEC model and concluded that fiber stiffness is unimportant and that it can be assumed that glass wool fibers are infinitely stiff without significant consequences (see Putland [6], Section 7.1.2, page 97 and *Fig. 10.11*, page 176). This conclusion can be debated if the fiber material is soft (e.g., like soft rubber, which has a high mass-to-stiffness ratio), causing resonances to occur at low frequencies, but the conclusion is assumed to be valid for PET wool. In addition, Putland concluded that the aerodynamic flow resistance is of higher importance than the thermodynamic relaxation (Putland [6], *Fig. 10.7, 10.12 – 10.14* and page 218). Putland called this the viscosity, while Leach called this the aerodynamic drag (as does Bradbury [7]).

Robinson [8] investigated fiberglass in a transmission line and concluded that a simplified model neglecting coupling between fibers provides good agreement with the measured data. This conclusion is based on the analysis of a transmission line; it should also be valid for closed and reflex boxes.

3.2. Calculation of an Enclosure Partially Filled with Damping Material

The aforementioned model is calculated with sample values to better illustrate and explain the condition of a partially filled enclosure. The thermodynamic and mechanical components of the model are treated separately.

3.2.1. Initial Definitions for the Model

The nomenclature largely follows that of Putland [5]. Initial definitions are given in Table 4.

Air pressure, p	101325 Pa
Air temperature, T	20 °C (= 293,15 K)
Air density, ρ_0	1,20 kg/m^3
Velocity of sound in air, c	344 m/s
Fill percentage, F_{pc}	15 % (F_r = 0,15)
Box volume, V_B	0,01 m^3 (10 liter)
Q_B (suggested)	100
Spec. heat ratio, γ (C_p/C_v)	1,4

Table 4 Defined air properties and inputs to the example.

The velocity of sound and air density specified here is based on a thermodynamic model, which uses the given pressure, temperature and 50 % RH (relative humidity) as inputs.

The fill percentage F_{pc} is not taken from Putland's paper but is introduced here to lay out the calculation for partially filled enclosures. The fill percentage is alternatively defined as a relative measure as $F_r = F_{pc} / 100 = 0,15$ in this case. While $F_{pc} > 100$ is allowed, the relative measure is defined as a value between $0 \leq F_r \leq$

1. In other words, for an enclosure with compressed fill, $F_r = 1$. Making this distinction between F_{pc} and F_r simplifies the algorithms.

For conversion to the electrical domain, the transducer parameters for the example driver in Section 2.2 are used: $Bl = 4{,}87$ T·m (or N/A) and $S_D = 0{,}0154$ m^2. When this driver is placed into a 10 liter closed box, the resonance frequency of the transducer in the box is $f_{SB} = 77$ Hz. In the case of a bass reflex box, the port tuning frequency f_P is used instead when specifying the frequency for further analysis (at whatever frequency Q_B is specified).

The suggested Q_B (box wall absorption) based on the observations by Small [3] can be changed as desired and is represented by R_B in *Fig. 4*, which basically serves as a "ceiling" to calculate losses in the enclosure such that the absorption Q-value does not tend towards infinity when the filling tends to zero. The Q_B value for an unlined enclosure found by Small should be re-evaluated with a transducer model that incorporates frequency-dependent damping for a better initial guess. This representation of wall damping is a simplification, neglecting for example panel resonances.

In practice, R_B can be used to fit the impedance of a model simulation to measurements of a leak free test box without damping. Then, much of R_B may stem from the damping behavior of the driver or the driver/box interface. R_B could be relocated to be parallel with L_{UA} only.

A quick analysis of a PET damping material named Acousto-Q has shown that the input data in Table 5 could be suitable for this type of damping material in the model by Leach (see Table 5).

The PET wool density ρ_{wool} was calculated from measurements of mass and volume. The solid PET density, ρ_f, and the specific heat capacity, C_f, were retrieved from a table of material data, whereas the fiber diameter was fitted to measured impedance data of a transducer in a box.

The air constants and fill amount in kilograms shown in Table 6 were calculated based on the above input.

It can be seen that κ and C_v are described by polynomial equations with respect to temperature T (in degrees Celsius), allowing for the specification of the temperature of the air in the enclosure. The amount of damping material F can be specified directly, if desired, but here it is calculated based on the specified fill percentage.

PET density (solid fiber), ρ_f	1400	kg/m^3	
PET wool density (uncomp.), ρ_{wool}	3,6	kg/m^3	
Spec. heat capacity of PET fiber, C_f	650	J/(kg K)	
Diameter of PET fiber, d_f	15 E-6	m	(= 15 μm)

Table 5 Fiber fill properties, tentative results.

Thermal conductivity of air	κ	$= 7{,}4342\text{E-}5 \cdot T + 0{,}02397$	= 0,0255	W/(m K)
Constant volume specific heat capacity of air	C_v	$= p / 101325 \cdot (0{,}0005 \cdot T^2 + 0{,}0069 \cdot T + 1004{,}9) / \gamma$	= 718	J/(kg K)
Constant pressure specific heat capacity of air	C_p	$= \gamma \cdot C_v$	= 1005,2	J/(kg K)
Thermal diffusivity of air	α	$= \kappa / (\rho_0 \cdot C_p)$	= 2,11 E-5	m^2/s
Fill	F	$= \rho_{wool} \cdot V_B \cdot F_{pc} / 100$	= 0,0054	kg

Table 6 Air constants and fill amount.

Solid fiber fill limit, F_{max}	$= \rho_f \cdot V_B$	= 14	kg	The enclosure is filled with solid PET, no air left in the enclosure
Uncompressed fill limit, F_{lim}	$= \rho_{wool} \cdot V_B$	= 0,036	kg	The enclosure is filled with uncompressed fiber wool
Fill factor limit, f_{lim}	$= \rho_{wool} / \rho_f$	= 0,00257		Fill factor when enclosure is filled with uncompressed fiber wool
m limit, m_{lim}	$= f_{lim}^{-1/2}$	= 19,7		Inverse fill factor (heat shed) limit at fill factor limit
τ limit, τ_{lim}	$= d_f^2 / (8 \cdot \alpha) \cdot (m_{lim}^2 - m_{lim}^{0,37}) \cdot \text{LN}((m_{lim} + 1) / 2)$	= 1,20 E-3	s	Upper limit transition time constant
f_C limit	$= 1 / (2 \pi \tau_{lim})$	= 132	Hz	Lower limit transition frequency where operation changes between adiabatic and isothermal condition

Table 7 Calculation of the limit cases.

Fill	$= F$	= 0,0054	kg	(from Table 6)
Fill factor, f	$= F / F_{max}$	= 386 E-6		(= 0,0386 %)
m	$= f^{-1/2}$	= 50,9		
τ_{fp}	$= d_f^2 / (8 \alpha) \cdot (m^2 - m^{0,37}) \cdot \text{LN}((m + 1) / 2)$	= 0,0112	s	(= 11,2 ms)
f_C	$= 1 / (2 \pi \tau_{fp})$	= 14,2	Hz	

Table 8 Calculation for the actual conditions, without corrections.

3.2.2. Thermodynamic Part of the Model

A number of limiting cases are calculated in Table 7. The actual conditions are listed in Table 8.

It should be noted that the inequality $\tau_{fp} > \tau_{lim}$ does not correlate with actual values, resulting in an f_C value lower than what is physically possible for the fibers to achieve. τ_{fp} should be changed to τ_{lim}. This means that whenever a partially filled enclosure is calculated, the limiting values of f, m and τ_{fp} (and f_C) are used as input values for the filled section of the enclosure.

For any situation with partial filling, the simplest approach is to apply the volume expansion found at F_{pc} = 100 % to the partial volume filled with damping material. This gives a volume expansion that follows a straight line down to F_{pc} = 0 %.

This is accomplished by defining $V_B = V_{BU} + V_{BF}$ as the net volume of the enclosure, which is 10 liters in this example. For the unfilled and filled part of the volume, $V_{BF} = V_B \cdot F_r$ is the filled volume, and $V_{BU} = V_B \cdot (1 - F_r)$ is the residual unfilled volume. For $F_{pc} > 100$ ($F_r = 1$), $V_{BF} = V_B$.

Leach's (and Putland's) model subtracts the volume of the fiber from V_{BF} in the calculation of C_{af}, which is usually a very small quantity, to account for the case in which the wool fiber material is compressed in the enclosure. At some point, when adding and compressing more damping material, the added solid fiber volume becomes larger than the gained volume expansion, and the effective volume starts to shrink (see *Fig. 5*). The model can, in theory, handle this situation until the enclosure is completely filled with solid material (fill factor $f = 1 = 100$ %).

For the specified model parameters in *Fig. 4*, the acoustic parameters shown in Table 9 were first calculated.

β	$= f \cdot \rho_f \cdot C_f / ((1-f) \cdot \rho_0 \cdot C_v)$		(Ratio of heat capacities, fiber versus air)
	$= f_{lim} \cdot \rho_f \cdot C_f / ((1-f_{lim}) \cdot \rho_0 \cdot C_v)$	= 2,72	(Use limit values when partially filled)
C_{ua}	$= V_{BU} / (\rho_0 \cdot c^2)$	= 59,9 nF	(Unfilled acoustic enclosure volume ≥ 0)
C_{af}	$= V_{BF} \cdot (1-f) / (\rho_0 \cdot c^2)$		(Filled acoustic enclosure volume ≥ 0)
	$= V_{BF} \cdot (1-f_{lim}) / (\rho_0 \cdot c^2)$	= 10,5 nF	(Use limit values when partially filled)
R_a	$= 1 / (2\pi \cdot f_{SB} \cdot Q_B \cdot (C_{af} + C_{ua}))$	= 294 Ω	(For vented box use f_P instead of f_{SB})
C_{th}	$= (\gamma - 1) \cdot \beta \cdot C_{af} / (\gamma + \beta)$	= 2,78 nF	(Apparent acoustic volume expansion)
R_{th}	$= \tau_{fp} / ((\gamma - 1) \cdot C_{af})$		(Thermodynamic damping)
	$= \tau_{lim} / ((\gamma - 1) \cdot C_{af})$	= 285 kΩ	(Use limit values when partially filled)

Table 9 Acoustical parameters for the thermodynamic part of the model and the unfilled section.

Finally, the electrical equivalents shown in Table 10 were calculated.

Further calculation shows that $V_B \cdot (1 - f) = 9{,}996$ liters (a bit less than the initial 10 liters because the fiber occupies a small volume) and $V_{TH} = 0{,}395$ liter, which is the effective volume expansion. The effective net volume becomes $V = V_B \cdot (1 - f) + V_{TH} = 10{,}391$ liters. These appear to be reasonable values, given that only 15 % of the enclosure volume is filled with damping material; 15 % of 10 liters = 1,5 liters, and within this 1,5 liters, the volume is expanded by approximately 26 % (approximately 0,39 liter).

L_{UA}	$= (Bl / S_D)^2 \cdot C_{ua}$	= 0,00599 H	(= 5,99 mH)
L_{AF}	$= (Bl / S_D)^2 \cdot C_{af}$	= 0,00105 H	(= 1,05 mH)
R_B	$= 1 / R_a \cdot (Bl / S_D)^2$	= 341 Ω	
L_{TH}	$= (Bl / S_D)^2 \cdot C_{th}$	= 0,000278 H	(= 0,278 mH)
R_{TH}	$= 1 / R_{th} \cdot (Bl / S_D)^2$	= 0,351 Ω	

Table 10 Electrical equivalents for the thermodynamic part of the model and the unfilled section.

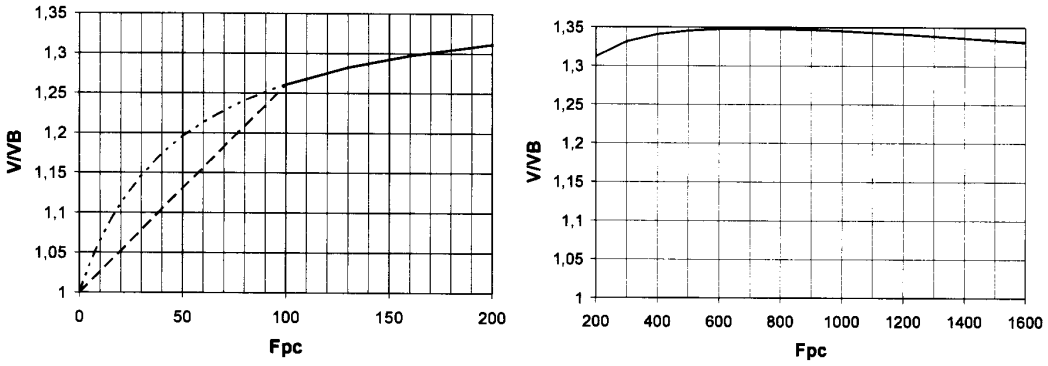

Figure 5 The normalized volume expansion V / V_B versus fill percentage F_{pc} (utilizing PET wool). The dash-dotted line represents the unmodified algorithm. The dashed line denotes linear scaling (from F_{pc} = 100 %, it is a straight line with 26 % volume expansion in the filled part of the volume). The solid line represents compressed wool. Relative volume expansion reaches its maximum at 1,348 when filling is 700 %.

The straight line in *Fig. 5* is a simplification. In reality, the damping material can be placed in numerous places of the box, such as behind the transducer, restricting the air flow from the transducer into the unfilled section, or away from the driver along the walls where air flow is limited; each position produces different results.

3.2.3. Mechanical Part of the Model

The mechanical model cannot be evaluated without including the geometrical aspects of the enclosure. Whereas Putland [6] utilized the FDEC method for handling geometric aspects, Leach [4] defined B as a geometrical factor.

Examples of typical design ratios are width × depth × height = 0,8 × 1 × 1,25 or, alternatively, the golden-section ratio 0,618 × 1 × 1,618. These ratios are close in value to those cited by Leach, although Leach defined the baffle area S_B based on the two largest dimensions, which the author believes is not the typical way of defining this parameter (the baffle is the side of the enclosure where the transducer is mounted). For the second example, more digits have been added (Leach specified 0,6 × 1 × 1,6). These ratios prevent multiple standing wave modes of lower order from appearing at (or near) the same frequency. At the same time, the baffle width × height = 1,0 in these cases, and the dimensions are easily given by the cubic root of the volume.

Leach assumed linearity between the extreme cases of an infinite baffle ($S_D << S_B$), where S_B = baffle area, and a small diameter tube with the driver located at the end ($S_D = S_B$), thus deriving ([4], Eq. 6):

$$B = \frac{d_B}{\sqrt{S_B}} \cdot \frac{\sqrt{\pi}}{3} \cdot \left(\frac{S_D}{S_B}\right)^{\frac{3}{2}} + \frac{8}{3\pi} \cdot \left(1 - \frac{S_D}{S_B}\right) \quad (8)$$

Combining Leach [4] and the above definitions, the geometry of the enclosure is defined first as the following:

$$V_B = V_{BU} + V_{BF} = S_B \cdot d_B \quad (9)$$

where d_B = depth of box, and S_B = baffle shadow area (the projected cross-sectional area).

The mass load from the air in the unfilled section is given by the following:

$$M_{ua} = \rho_0 \cdot \frac{d_B}{3 \cdot S_B} \cdot (1 - F_r) = \rho_0 \cdot \frac{V_{BU}}{3 \cdot S_B^{\,2}} \quad (10)$$

According to Leach, the mass load from the air in the fiber-filled section is given by the following:

$$M_{af} = \frac{B}{\sqrt{\pi \cdot S_D}} \cdot \rho_0 \cdot (1 - f) \quad (11\text{ a})$$

$$= F_r \cdot \frac{B}{\sqrt{\pi \cdot S_D}} \cdot \rho_0 \cdot (1 - f) \quad (11\text{ b})$$

In Equation 11, the volume of the fiber fill is excluded by including $(1 - f)$. Putland stated that this should not be excluded ([6], page 97), though it can be rationalized by observing at Equation 12. M_{af} becomes C_{AF} in the electrical model. Equation 11b is valid for a partially filled enclosure.

The mass portion of the air in the enclosure, $M_{ua} + M_{af}$, which loads the transducer, is primarily composed of the air near the transducer, whereas the air near the enclosure walls does not move and therefore does not factor into the mass loading of the driver (Putland, [6], Section 7.3, page 117).

The mass load from the fibers in the fiber-filled section is given by Equation 12.

$$M_{mf} = \frac{B}{\sqrt{\pi \cdot S_D}} \cdot \rho_f \cdot f \quad (12\text{ a})$$

$$= F_r \cdot \frac{B}{\sqrt{\pi \cdot S_D}} \cdot \rho_f \cdot f \quad (12\text{ b})$$

The fill ratio, F_r, is used in Equation 10, 11 and 12 as a decoupling of mass loading because the residual amount of filling cannot be assumed to fully load the transducer.

The aerodynamic flow resistance through the fiber-filled section is given by Equation 13.

$$R_{af} = B \cdot \frac{n}{\sqrt{\pi \cdot S_D}} \cdot \delta \quad (13\text{ a})$$

$$= B \cdot \frac{1-f}{\sqrt{\pi \cdot S_D}} \cdot \lambda \quad (13\text{ b})$$

where the relationship $n \cdot \delta = (1 - f) \cdot \lambda$ is used (Putland [6], page 97). λ is the pneumatic resistivity ([6], page 98) and is in other cases named R_f, see Robinson [8] and R_{cr}, see Tarnow [9]. λ is evaluated below.

Putland [6] defined λ in accordance with Bradbury [7]. Robinson [8] has shown that Tarnow [9] provided a more recent expression based on a theoretical physical analysis.

Equation 14a, which is taken directly from Tarnow [9, 10], is valid when the air flow direction is perpendicular to the fibers (the subscript 'cr' means cross-flow, random fiber distance); in Equation 14b, the expression is adapted to the nomenclature used in the present paper:

$$R_{cr} = \frac{4\pi\eta}{b^2 \cdot (0{,}640 \cdot LN(1/d) - 0{,}737 + d)} \quad (14\text{ a})$$

$$= \frac{16 \cdot \eta}{d_f^{\,2}} \cdot \frac{f}{0{,}640 \cdot LN(1/f) - 0{,}737 + f} \quad (14\text{ b})$$

Tarnow defined d as the volume concentration of cylinders (in our case the fill factor = f) and b as the square root of the area per fiber (or mean spacing between plates), which is redefined as $b^2 = \pi\, a_f^2 / f$, where a_f is the radius of the fiber (d_f = fiber diameter). The following dynamic viscosity of dry air is used as a simplification of Kadoya et al. [11] (see Putland [12] and [6], Eq. 9.10 page 144):

$$\eta = 18{,}57 \cdot 10^{-6} \cdot \left(\frac{T}{300K}\right)^{0{,}7829} [Pa \cdot s] \quad (15)$$

The simplified equation for η is valid around normal room temperatures. Equation 15 is within 1 % of the value determined by Kadoya et al. from -60 to +150 °C, within 0,1 % from -4 to +58 °C and only deviates by 0,0047 % at +25 °C. These models are valid for dry air. If one can accept the deviations, the approximate Equation 15 by Putland offers a simpler expression.

Equation 14 is the one utilized by Robinson. It concerns only air flow perpendicular to the fibers, presumably because this is the way Robinson applied the glass wool material in his transmission line; however, Tarnow has also provided a mathematical solution for air flow along

(parallel to) the fibers (subscript 'lr' means longitudinal-flow, random fiber distance), see Equation 16.

$$R_{lr} = \frac{R_{cr}}{2} = \frac{4\pi\eta}{b^2 \cdot (1{,}280 \cdot LN(1/d) - 1{,}474 + 2 \cdot d} \quad (16\text{ a})$$

$$= \frac{16 \cdot \eta}{d_f^{\,2}} \cdot \frac{f}{1{,}280 \cdot LN(1/f) - 1{,}474 + 2 \cdot f} \quad (16\text{ b})$$

Flow along the fibers is easier than across the fibers by a factor of 2. The equations are approximate (but exact for plates). Tarnow investigated the results of his theoretical derivations with a number of known measurements and numerical approximations. Tarnow concluded that his findings are within 20 % of the previous findings of other authors. Tarnow claimed that for acoustic materials, fill factors < 0,02 are expected, and this simplifies computations (by removing a squared term, d^2, from the denominator). A fill factor of 0,02 for PET wool in a 10-liter enclosure is equivalent to 280 grams of PET damping material (F_{pc} = 778 %), and it may be concluded that, at least for PET wool material, Tarnow is correct (see *Fig. 5*).

Tarnow studied glass wool, which is an anisotropic material in which layers of glass wool are separable and fibers are not completely random (but in layers), whereas PET wool is typically of more random nature, without anisotropy. Therefore, Equations 14 and 16 are re-evaluated to represent a more uniform (3-dimensional purely random) orientation of the fibers.

When looking at glass wool along its separable layers (two out of three directions), half of the fibers are oriented perpendicular to the direction of air flow and half are oriented along the axis of air flow. When looking into the glass wool from the third direction, all fibers are perpendicular to the air flow. When combining R_{cr} and R_{lr}, they should be combined in ratios of 2/3 R_{cr} and 1/3 R_{lr} as follows:

$$R_f = \lambda = R_{cr}^{\,2/3} \cdot R_{lr}^{\,1/3} \quad (17\text{ a})$$

$$= \frac{16 \cdot \eta}{d_f^{\,2}} \cdot \frac{f}{0{,}806 \cdot LN(1/f) - 0{,}929 + 1{,}26 \cdot f} \quad (17\text{ b})$$

Equation 17 assumes that when the fibers are not all perpendicular or all in-plane but are between these two extremes, the interpolation as described above can be applied as an average expression. Tarnow [10] used a similar approach, converting resistance to conductivity (G = 1/R), but his investigation was focused on glass wool, which is heavily non-homogenous and anisotropic; he concluded that for glass wool, practical measures show that the overall resistance is lower than that predicted by this method. For PET wool, the method used to derive Equation 17 is valid.

Tarnow also found that in glass wool, the fibers have a tendency to form pairs; hence, the apparent fiber diameter, when fitting data, seems larger than what can be measured for a single fiber. This is partially due to the way glass wool is manufactured on a conveyor belt, which aligns fibers in particular directions. Less randomness may furthermore become the result of heavy compression, where fibers are forced to align at higher fill factors. Tarnow found good agreement with fill factors up to 0.02, but he has studied fill factors as

high as 0.1 and found acceptable agreement between his theory and measurements.

The equation for λ as defined above in Equation 17b derived from Tarnow [9, 10] is chosen. This is partially because Robinson has investigated the two options and found a limited agreement between the two, while Putland clearly stated [6] that λ is the least accurately defined parameter in his thesis, and Bradbury presented this only as a tentative expression. Given that Tarnow's derivation is 20 years newer than Bradbury's, is based on the random distance between fibers, and has been verified against measurements and numerical solutions, it is assumed to be better. λ is still not accurately defined, and therefore R_{af} (Equation 13), is given with significant uncertainty.

If Bradbury's expression is used, $\lambda = 36$, whereas if that of Tarnow is used, $R_{lr} = 58$ and $R_{cr} = 116$ (the combined $R_f = \lambda = 92$).

The acoustical properties are converted to their electrical equivalents in Table 11.

C_{UA}	$= (S_D / Bl)^2 \cdot M_{ua}$
C_{AF}	$= (S_D / Bl)^2 \cdot M_{af}$
C_{MF}	$= (S_D / Bl)^2 \cdot M_{mf}$
R_{AF}	$= (Bl / S_D)^2 / R_{af}$

Table 11 The electrical equivalent parameters for the mechanical part of the fiber model.

3.3. Example Calculation

Input from Table 4 is used:

Air temperature, T	20 °C (= 293,15 K)
Air density, ρ_0	1,20 kg/m^3
Fill percentage, F_{pc}	15 % (F_r = 0,15)
Box volume, V_B	0,01 m^3 (10 liter)

The dynamic viscosity of (dry) air, η, is calculated as follows:

$\eta = 18{,}57 \cdot 10^{-6} \cdot (T/300\ \text{K})^{0{,}7829} = 1{,}82372 \cdot 10^{-5}$ Pa s (= Ns/m^2 or kg/(m·s)) (= 18,2 μPa s)

Previously defined fiber properties (from Table 5):

PET density (solid fiber), ρ_f	1400	kg/m^3	
PET wool density (uncomp.), ρ_{wool}	3,6	kg/m^3	
Diameter of PET fiber, d_f	15 E-6	m	(= 15 μm)

Previously defined transducer properties (from Table 1):

Bl	4,87 Tm (or N/A)
S_D	0,0154 m^2 (= 154 cm^2)

Furthermore, the following parameters have been previously specified for the partially filled enclosure (from Table 7), and V_{BU} and V_{BF} are calculated:

$f_{lim} = \rho_{wool} / \rho_f = 0{,}00257$

$f = F / F_{max} (= F_r \cdot f_{lim}) = 0{,}000386$

$V_{BU} = (1 - F_r) \cdot V_B = 0{,}0085$ m^3

$V_{BF} = F_r \cdot V_B = 0{,}0015$ m^3

$h_B = 1{,}25 \cdot V_B^{1/3}$ = 0,269 304 m (= 26,9 cm)

The dimensions and properties of the box are calculated: $S_B = w_B \cdot h_B$ = 0,046 416 m² (= 464 cm²)

$w_B = 0{,}8 \cdot V_B^{1/3}$ = 0,172 355 m (= 17,2 cm)

$d_B = 1{,}0 \cdot V_B^{1/3}$ = 0,215 443 m (= 21,5 cm)

$B = d_B / \sqrt{S_B} \cdot \sqrt{\pi} / 3 \cdot (S_D / S_B)^{3/2} + 8 / (3 \cdot \pi) \cdot (1 - S_D / S_B)$ = 0,680 111

The mechanical model parameters are calculated (in the acoustic domain):

$M_{ua} = \rho_0 \cdot V_{BU} / (3 \cdot S_B^2)$ = 1,578 kg/m⁴

$M_{af} = F_r \cdot B / \sqrt{(\pi \cdot S_D)} \cdot \rho_0 \cdot (1 - f)$ = 0,556 kg/m⁴

$M_{mf} = F_r \cdot B / \sqrt{(\pi \cdot S_D)} \cdot \rho_f \cdot f$ = 0,250 kg/m⁴

$R_{af} = B \cdot (1 - f) / \sqrt{(\pi \cdot S_D)} \cdot 16\,\eta / (d_f^2) \cdot f / (0{,}806 \cdot \mathrm{LN}(1/f) - 0{,}929 + 1{,}26 \cdot f)$ = 286 Ns/m⁵

The electrical equivalents are calculated:

$C_{UA} = (S_D / Bl)^2 \cdot M_{ua}$ = 15,78 · 10⁻⁶ Farad (= 16 µF)

$C_{AF} = (S_D / Bl)^2 \cdot M_{af}$ = 5,56 · 10⁻⁶ Farad (= 5,6 µF)

$C_{MF} = (S_D / Bl)^2 \cdot M_{mf}$ = 2,50 · 10⁻⁶ Farad (= 2,5 µF)

$R_{AF} = (Bl / S_D)^2 / R_{af}$ = 350 Ω

The total capacitance of all of the capacitors is 23,8 µF, which in this particular example is equivalent to 0,56 grams of added mass load from inside the box; however, it should be noted that the mass loading is distributed to various places in the model.

4. CONCLUSION

The present paper reveals that frequency-dependent damping is a significant factor in conventional transducers, including those of the low-damping type that constitute today's standard. Moreover, it is shown that frequency-dependent damping influences how loudspeaker enclosure losses and their magnitude and importance are understood, shifting focus from leakage (Q_L) to absorption (Q_A).

Furthermore, it has been shown that applying frequency-dependent damping should change how traditional engineering practices are executed, from treating arbitrary losses to treating losses defined by a physical model. A model created for this purpose is presented here to help utilize frequency-dependent damping in transducers for the development of more accurate simulations of loudspeaker enclosures. A method for handling the case of a partially filled enclosure has also been shown.

The simplified circuit model presented here cannot predict the desired suppression of resonances in the mid-band or other higher-order effects, e.g., panel resonances. It only approximately predicts the undesired side effect of damping in the low-frequency rolloff.

Models of damping materials have existed for decades, but not yet been successfully implemented. This is simply because the commonly used transducer models defeat any potential improvement in accuracy.

5. FUTURE WORK

Future work will include verification for the presented enclosure absorption loss model.

In addition, a virtually loss-less test box has been built and will also be tested. Parameters for a driver can then be derived by free air and added mass curve fitting. The driver will then be measured in the box, to find new typical "best case" guideline values for absorption and leakage, which are suitable for the model presented in this paper.

The absorption Q as defined by Small is a result of multiple loss effects (see $R_B + R_{TH} + R_{AF}$ in *Fig. 4*) when damping material is applied. To evaluate which Q_A is typically expected, an enclosure should be simulated with and without damping material and verified against measurements. The change in peak impedance Z_{RES} should yield a lumped value for Q_A due to damping material.

One question remains to be answered: Can the model of enclosure damping be improved by applying frequency-dependent damping?

6. ACKNOWLEDGEMENTS

The author gratefully acknowledges Knud Thorborg for reviewing this paper, especially the first half related to the description of the transducer.

The author gratefully acknowledges Christopher J. Struck, of CJS Labs for reviewing this paper and providing valuable comments and suggestions.

The author wishes to extend a special thanks to Gavin R. Putland for reviewing this paper, especially the second half related to the damping material. He helped establish the mechanical model for a partially filled enclosure, *Fig. 3*, and he directed the author towards his PhD thesis for answers, which, with the model by Leach, became the basis of Section 3. Without his help, the third section of this paper would not have been the same.

7. REFERENCES

[1] K. Thorborg, C. Tinggaard, F. Agerkvist and C. Futtrup, "Frequency Dependence of Damping and Compliance in Loudspeaker Suspensions," J. Audio Eng. Soc., vol. 58, pp. 472-486 (June 2010)

[2] K. Thorborg, U. Skov and C. Futtrup, "Electro-dynamic Transducer Model Incorporating Semi-Inductance and Means for Shorting AC Magnetization," J. Audio Eng. Soc. (to be published)

[3] Richard H. Small, "Vented-Box Loudspeaker Systems, Part 1: Small-Signal Analysis," J. Audio Eng. Soc., vol. 21, pp. 363-372 (June 1973)

[4] W. Marshall Leach, Jr., "Electroacoustic-Analogous Circuit Models for Filled Enclosures," J. Audio Eng. Soc., vol. 37, pp. 586-592 (July/August 1989)

[5] Gavin R. Putland, "Thermal Time Constants and Dynamic Compressibility of Air in Fiber-Filled Loudspeaker Enclosures," J. Audio Eng. Soc., vol. 46, pp. 139-151 (March 1998)

[6] Gavin Richard Putland, "Modeling of Horns and Enclosures for Loudspeakers," PhD thesis,

Department of Electrical and Computer Engineering, University of Queensland, 1996.

[7] L. J. S. Bradbury, "The Use of Fibrous Materials in Loudspeaker Enclosures," J. Audio Eng. Soc., vol. 24, pp. 390-398 (April1976)

[8] Robert Allen Robinson, Jr., "An Electroacoustic Analysis Of Transmission Line Loudspeakers," PhD thesis, School of Electrical and Computer Engineering, Georgia Institute of Technology, 2007.

[9] Viggo Tarnow, "Airflow resistivity of models of fibrous acoustical materials," J. Acoust. Soc. Am., vol. 100, pp. 3706-3713, Dec. 1996

[10] Viggo Tarnow, "Measured anisotropic air flow resistivity and sound attenuation of glass wool," J. Acoust. Soc. Am., vol. 111, pp. 2735-2739, June 2002

[11] K. Kadoya, N. Matsunaga & A. Nagashima: "Viscosity and Thermal Conductivity of Dry Air in the Gaseous Phase", J. Physical and Chemical Reference Data, vol. 14, pp. 947–70 (1985)

[12] Gavin R. Putland, "Acoustic Properties of Air versus Temperature and Pressure," J. Audio Eng. Soc., vol. 42, pp. 927-933 (November 1994)